Influence of doped charge transport layers on efficient perovskite solar cells.

Jorge Avila[1], Lidon Gil-Escrig[2], Pablo P. Boix[1], Michele Sessolo[1], Steve Albrecht[2] and Henk J. Bolink*[1]*

[1]Instituto de Ciencia Molecular, Universidad de Valencia, C/ J. Beltrán 2, 46980, Paterna, Spain
[2]Helmholtz-Zentrum Berlin für Materialien und Energie GmbH, Young Investigator Group for Perovskite Tandem Solar Cells, Kekuléstraße 5, 12489 Berlin, Germany

Supporting Information

Materials. Photolithographically patterned ITO coated glass substrates were purchased from Naranjo Substrates (www.naranjosubstrates.com). 2,2'-(Perfluoronaphthalene-2,6-diylidene) dimalononitrile (F_6-TCNNQ), N4,N4,N4",N4"-tetra([1,1'-biphenyl]-4-yl)-[1,1':4',1"-terphenyl]-4,4"-diamine (TaTm) and N1,N4-bis(tri-p-tolylphosphoranylidene)benzene-1,4-diamine (PhIm) were provided from Novaled GmbH. Fullerene (C_{60}) was purchased from sigma Aldrich and 2,9-Dimethyl-4,7-diphenyl-1,10-phenanthroline (BCP) from Lumtec. PbI_2 was purchased from Tokyo Chemical Industry CO (TCI), and CH_3NH_3I (MAI) from Lumtec**.**

Device preparation. ITO-coated glass substrates were subsequently cleaned with soap, water and isopropanol in an ultrasonic bath, followed by UV-ozone treatment. They were transferred to a vacuum chamber integrated into a nitrogen-filled glovebox (MBraun, H_2O and O_2 < 0.1 ppm) and evacuated to a pressure of $1 \cdot 10^{-6}$ mbar. The vacuum chamber uses a turbomolecular pump (Pfeiffer TMH 261P, DN 100 ISO-K, 3P) coupled to a scroll pump. The vacuum chamber is equipped with six temperature controlled evaporation sources (Creaphys) fitted with ceramic crucibles. The sources were directed upwards with

an angle of approximately 90º with respect to the bottom of the evaporator. The substrate holder to evaporation sources distance is approximately 20 cm. Three quartz crystal microbalance (QCM) sensors are used, two monitoring the deposition rate of each evaporation source and a third one close to the substrate holder monitoring the total deposition rate. For thickness calibration, we first individually sublimed the charge transport materials and their dopants (TaTm and F_6-TCNNQ, C_{60} and PhIm). A calibration factor was obtained by comparing the thickness inferred from the QCM sensors with that measured with a mechanical profilometer (Ambios XP1). Then these materials were co-sublimed at temperatures ranging from 135-160 ºC for the dopants to 250 ºC for the pure charge transport molecules, and the evaporation rate was controlled by separate QCM sensors and adjusted to obtain the desired doping concentration. In general, the deposition rate for TaTm and C_{60} was kept constant at 0.8 Å s^{-1} while varying the deposition rate of the dopants during co-deposition. Pure TaTm, F_6-TCNNQ, BCP and C_{60} layers were deposited at a rate of 0.5 Å s^{-1}.

For devices A and D, 40 nm of the p-doped hole-transport layer (TaTm: F_6-TCNNQ) capped with 10 nm of the pure TaTm were deposited. For devices B, only 10 nm of TaTm was evaporated. For devices C and E, a thin (2.5 nm) layer of the molecule F_6-TCNNQ is deposited on top of the ITO prior to depositing the layer of TaTm. Once completed this deposition, the chamber was vented with dry N_2 to replace the HTL crucibles with those containing the starting materials for the perovskite deposition, PbI_2 and CH_3NH_3I. The vacuum chamber was evacuated again to a pressure of 10^{-6} mbar, and the perovskite films were then obtained by co-deposition of the two precursors. The use of clean QCM sensors for the perovskite evaporation is important to avoid false readings due to perovskite formation on the sensor. For a more accurate deposition the density of PbI_2 (6.16 g/cm^3) is set in the equipment. For CH_3NH_3I the density is assumed to be 1 g/cm^3. And the z-factor for both materials is set to 1. The calibration of the deposition rate for the CH_3NH_3I was found to be difficult due to non-uniform layers and the soft nature of the material which impeded accurate thickness measurements. Hence, the source temperature of the CH_3NH_3I was kept constant at 70 ºC and the CH_3NH_3I:PbI_2 ratio was controlled off line using grazing incident x-ray diffraction by adjusting the PbI_2 deposition temperature. The optimum deposition temperatures were found to be 250 ºC for the PbI_2 and 70 ºC for the CH_3NH_3I. After deposition of a 500 nm thick perovskite film, the chamber was vented, and the crucibles replaced with those containing the electron-transport materials and

evacuated again to a pressure of 10^{-6} mbar. The devices were completed depositing a film of pure C_{60} (10 nm for devices A, B and C; 25 nm for devices D and E). In the case of devices A, B and C, 40 nm of the n-doped hole-transport layer (C_{60}: PhIm) was evaporated. On devices D and E, the doped C_{60} layer is substituted by a thin layer (8 nm) of BCP. Afterwards the metal top contact (Ag, 100 nm thick) was deposited.

Characterization. Grazing incident X-ray diffraction (GIXRD) pattern were collected at room temperature on an Empyrean PANanalytical powder diffractometer using the Cu Kα1 radiation. Typically, three consecutive measurements were collected and averaged into single spectra. Scanning Electron Microscopy (SEM) images were performed on a Hitachi S-4800 microscope operating at an accelerating voltage of 2 kV over Platinum - metallized samples. Absorption spectra were collected using a fiber optics based Avantes Avaspec2048 Spectrometer. Characterization of the solar cells was performed as follows. The external quantum efficiency (EQE) was estimated using the cell response at different wavelength (measured with a white light halogen lamp in combination with band-pass filters), where the solar spectrum mismatch is corrected using a calibrated Silicon reference cell (MiniSun simulator by ECN, the Netherlands). The current density-voltage (J-V) characteristics were obtained using a Keithley 2400 source measure unit and under white light illumination, and the short circuit current density was corrected considering the device EQE. The electrical characterization was validated using a solar simulator by Abet Technologies (model 10500 with an AM1.5G xenon lamp as the light source). Before each measurement, the exact light intensity was determined using a calibrated Si reference diode equipped with an infrared cut-off filter (KG-3, Schott). The J-V curves were recorded between -0.2 and 1.2 V with 0.01 V steps, integrating the signal for 20 ms after a 10 ms delay. This corresponds to a speed of about 0.3 V s^{-1}. The layout used to test the solar cells has four equal areas (0.04 cm^2, defined as the overlap between the ITO and the top metal contact) and measured through a shadow mask with 0.01 cm^2 aperture.

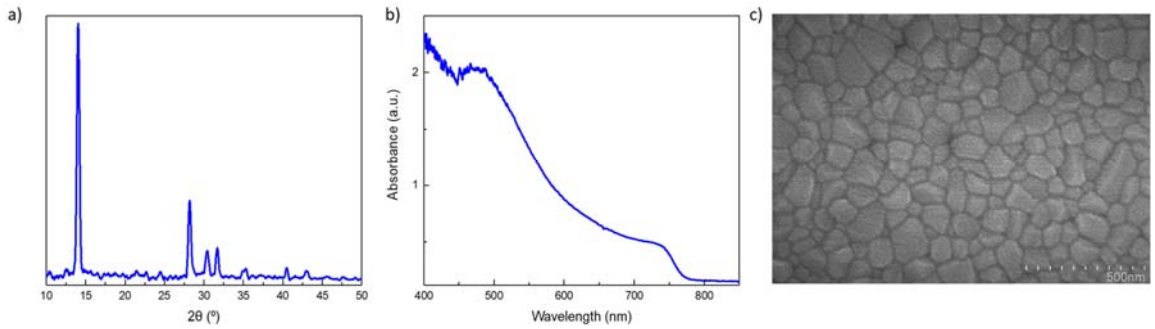

Fig S1 (a) GIXRD pattern, (b) optical absorbance and (c) surface SEM picture of the vacuum deposited $CH_3NH_3PbI_3$ thin films for devices preparation.

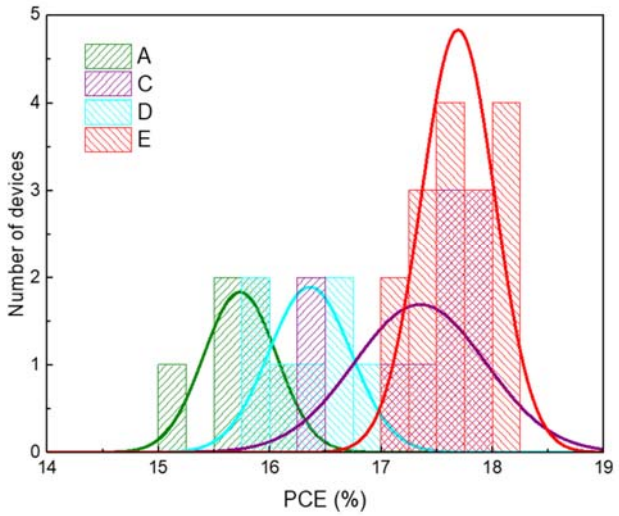

Fig S2 Statistic of the PCE measured for each type of devices. Solid lines represent the Gaussian distribution fitting for the PCE.

Table S1 Statistical distribution of J-V parameters of devices measured under standard AM1.5G illumination.

	PCE (%)	**J_{sc} (mA/cm^2)**	**V_{oc} (mV)**	**FF (%)**
A	15.7 ± 0.3	19.6 ± 1.1	1069 ± 8	75 ± 3
B	5.4	18.8	1032	27.9

C	17.4 ± 0.6	20.7 ± 0.5	1061 ± 13	79.1 ± 1.6
D	16.4 ± 0.4	19.2 ± 0.5	1058 ± 7	80.5 ± 1.7
E	17.7 ± 0.3	20.6 ± 0.4	1065 ± 5	80.7 ± 1.0

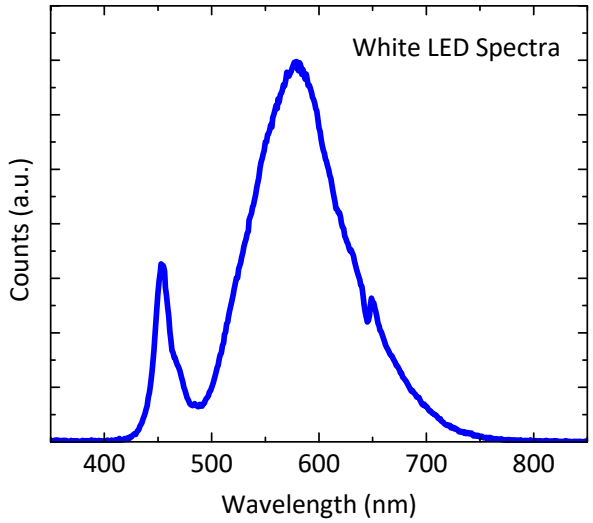

Fig S3 Optical emission spectrum of the white LED used to illuminate the solar cells during life time measurements.

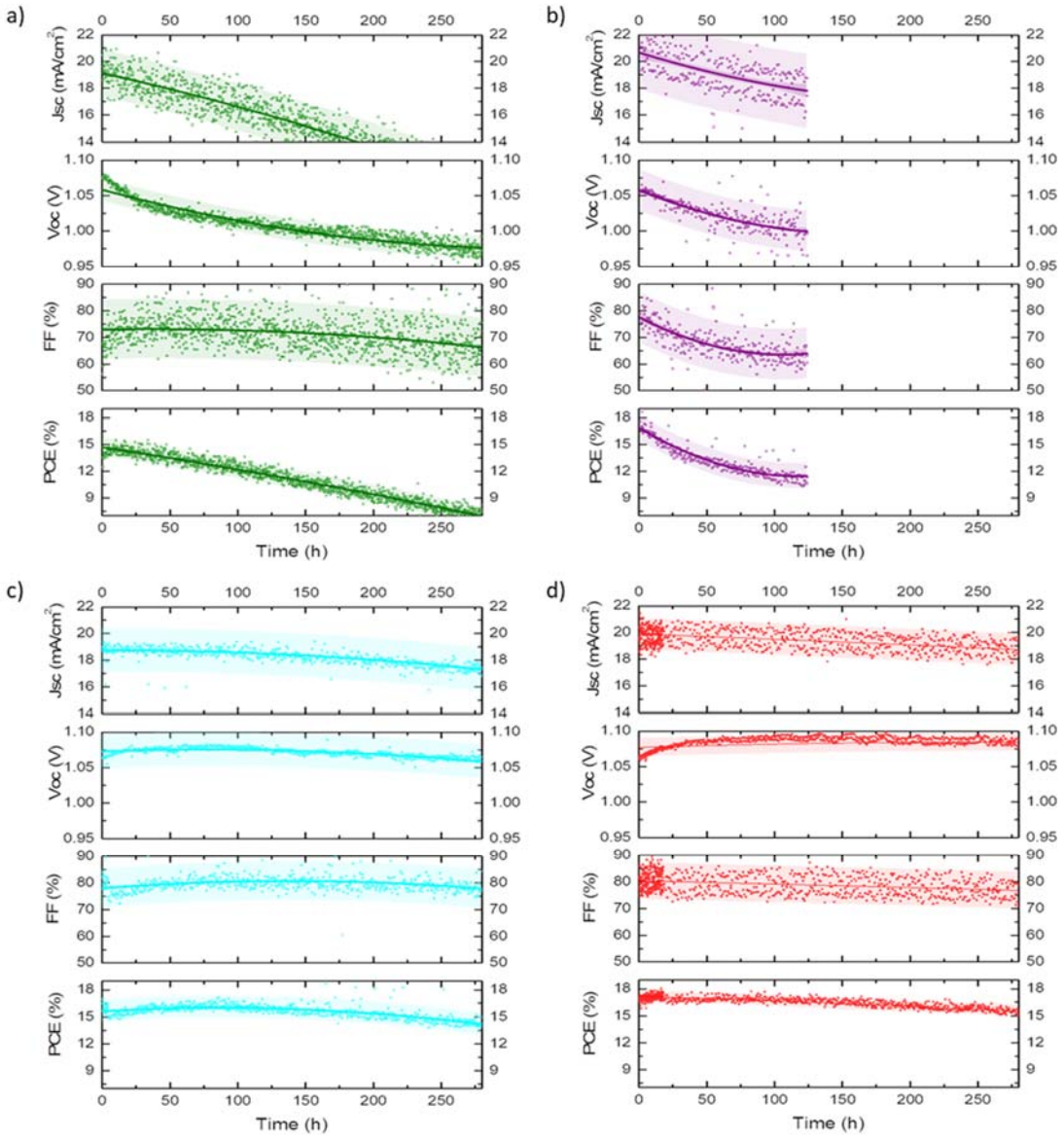

Figure S4 J-V characteristic parameters versus time measured under continuous illumination for devices A(a), C(b), D(c) and E(d).

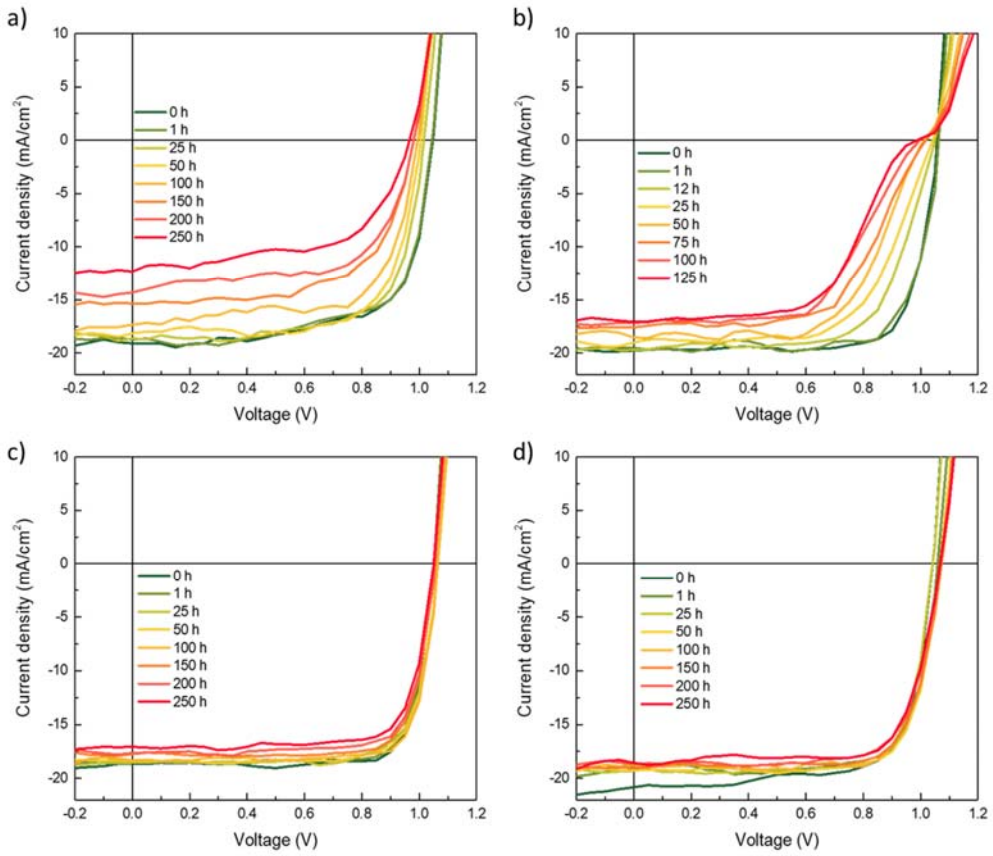

Figure S5 J-V curves measured at various times under continuous illumination for devices A(a), C(b), D(c) and E(d).